 CMES, vol.42, no.2, pp.107-129, 2009

A fast Monte-Carlo Solver for Phonon Transport in Nanostructured Semiconductors

Mei-Jiau Huang[1], Tung-Chun Tsai[1], Liang-Chun Liu[1]
Ming-shan Jeng[2] and Chang-Chung Yang[2]

Abstract: We develop a Monte-Carlo simulator for phonon transport in nanostructured semiconductors, which solves the phonon Boltzmann transport equation under the gray medium approximation. Proper physical models for the phonon transmission/reflection at an interface between two different materials and proper numerical boundary conditions are designed and implemented carefully. Most of all, we take advantage of geometric symmetry that exists in a system to reduce the computational amount. The validity and accuracy of the proposed MC solver was successfully verified via a 1D transient conduction problem and the cross-plane (1D) and in-plane (2D) phonon transport problems associated with Si/Ge superlattice thin films.

Keywords: Monte-Carlo simulator, phonon transport, gray medium approximation, nanostructures.

1 Introduction

Low-dimensional materials such as superlattice thin films, nanowires, and nanoparticle composites, received great attention over the past two decades for their potential application in thermoelectric devices and microelectronics (Venkatasubramanian, Siivola, Colpitts, and O'Quinn, 2001; Dresselhaus, Chen, Tang, Yang, Lee, Wang, Ren, Fleurial, Gogna, 2007; Hochbaum, Chen, Delgado, Liang, Garnett, Najarian, Majumdar, and Yang, 2008). In particular, it is found the largely reduced thermal conductivity of these nanostructured materials comes mainly from the sequential interface scattering of phonons rather than the coherent superposition of phonon waves. Analytic thermal conductivity models are usually developed based on the phonon Boltzmann transport equation (PBTE). Commonly considered scattering mechanisms include the three-phonon Umklapp scattering,

[1] Mechanical Engineering Department, National Taiwan University, Taipei, Taiwan
[2] Energy & Environment Laboratories, Industrial Technology Research Institute, Hsinchu, Taiwan

the mass-difference scattering, the phonon-electron scattering, the boundary scattering, and so on (Ziman, 2001); the Matthiessen's rule is then employed to sum up these scattering rates. Above all, two boundary effects deserve great attention. One is the modification of the phonon dispersion due to the spatial confinement (Khitun, Balandin, and Wang, 1999; Balandin and Wang, 1998; Kiselev and Kim, 2000) and the other is the change in the non-equilibrium phonon distribution due to the totally or partially diffuse boundary (Hyldgaard and Mahan, 1996; Chen, 1997, Chen, 1998; Walkauskas, Broido, Kempa, and Reinecke, 1999). Some investigations took both effects into consideration (Zou and Balandin, 2001; Huang, Chong, and Chang, 2006; Huang, Chang, Chong, 2007). Evgrafov, Maute, Yang, and Dunn (2009) demonstrated the differences between the optimal distributions of two constituents predicted by Fourier's law and kinetic theory, which give the maximization of a temperature difference between certain points. Theoretical studies are available nonetheless only for systems with simple geometry and involve more or less unrealistic assumptions. The analysis becomes intractable when the materials possess complicated nanostructures and when realistic conditions such as deficiency must be taken into consideration. Based on the same physical models, numerical solutions of the associated governing equations are naturally the next choice.

Over the last two decades, there has been tremendous advancement in the development of solution techniques for the BTE of charge carriers. Limited progress nonetheless has been made in the BTE solutions of phonons. Among all, the Monte Carlo simulation has a significant advantage that it allows the study of quasiparticle transport in peculiar geometry from nano- to micro- scale over other direct Boltzmann equation solvers such as the discrete ordinate method (Yang, Chen, Laroche, and Taur, 2005), the finite volume method (Murthy and Mathur, 2002), traditional molecular dynamics simulation (Hoover, 1983; Gomes, Madrid, Goicochea, and Amon, 2006; Volz, Saulnier, Chen, Beauchamp, 2000), and combined methods (Shen and Atluri, 2004). Peterson (1994) first proposed to simulate the phonon flows in solids by Monte-Carlo (MC) method. The boundary cells were maintained at constant temperatures by updating the local phonon properties every time step. The phonon distribution was discretized in the space as well as in the frequency domain. Phonons were then drifted at their group velocity and scattered based on a constant mean free path. Mazumder and Majumdar (2001) proposed a scattering probability that is a function of the frequency and the local temperature. The N and U processes were lumped into a single relaxation time. The scattering by impurities was treated in isolation. A genetic algorithm was carefully designed by Chen, Li, Lukes, and Majumdar (2005), in which both the momentum and the energy are conserved during N processes and only energy is conserved

during U processes. Moreover, the constant-temperature boundary condition was maintained by injecting phonons carrying properties at the prescribed temperatures from the boundaries. It was found the confinement effect is significant when the Si nanowire diameter is reduced to the sub-100 nm scale and a confined phonon dispersion should be used in order to accurately evaluate nanowire thermal conductivity. Lacroix, Joulain, and Lemonnier (2005) proposed a new distribution function accounting for the collision processes. Phonons' directions are not changed if they suffer an N process to approximately preserve momentum. Yang, Chen, Laroche, and Taur (2005) proposed a ballistic-diffusive heat conduction equation (BDE) and solved it via the discrete ordinate method. A better prediction from BDE, compared to the prediction from the phonon Boltzmann equation, was claimed. Escobar, Ghar, Jhon, and Amon (2006) developed a gray lattice Boltzmann method under the Debye assumption. The multi-length-and-time scale heat conduction in thin films from continuum to sub-continuum regimes was investigated. Jeng, Yang, Song, and Chen (2008) solved the gray-phonon Boltzmann equation also via the MC method. Averaged phonon properties over frequency at the local temperature (gray medium approximation) and a lumped relaxation time characterizing all kinds of scattering mechanisms were used to simplify the simulations. Their investigations suggested the interfacial area per unit volume is the key parameter that characterizes the size effect on the thermal conductivity of nanocomposites. Tian and Yang (2007), based on the same numerical tool, found the thermal conductivity of compacted Si embedded with Ge nanoparticles is around half of that of compacted Si embedded with Ge nanowires at the same atomic composition and characteristic size. They (2008) further demonstrated that when the characteristic size of the nanoparticles in the nanocomposites is comparable to or smaller than the phonon mean free path, the thermal conductivity of the nanoparticle composites significantly deviates from the predictions of the percolation theory due to the phonon scattering at interfaces.

Although the accuracy may be scarified a little, the gray medium approximation does save a lot of computational time and the MC tool becomes a quick analyzer for the design and choice of processing parameters in the preparation of nanostructured materials. In this study, we aim at improving the MC tool developed by Jeng, Yang, Song, and Chen (2008) for an even higher computational efficiency by taking advantage of the geometric symmetry in a system and for a higher accuracy by developing more physically reasonable models for heterogeneous interfaces as well as boundaries. The rest of this paper is arranged as follows. In Sec. 2, we introduce the physical models adopted in the present work. We discuss the development of the proposed numerical boundary condition and the usage of the geometric symmetry in Sec.3. The so-developed fast MC solver is first verified through a transient

problem and then applied to the cross-plane and in-plane phonon transports in a Si/Ge superlattice thin film in Sec.4. Conclusions are given at last in Sec.5.

2 Physical models

2.1 Phonon Boltzmann transport equation

The PBTE is written as follows

$$\frac{\partial n}{\partial t} + \vec{v}_g \cdot \nabla n = (\partial n/\partial t)_s \tag{1}$$

where n is the phonon population having a group velocity $\vec{v}_g$ and $(\partial n/\partial t)_s$ is the intrinsic scattering rate. To compute the intrinsic scattering rate, a single relaxation time (τ) characterizing all kinds of scatterings is assumed. The possibility that a phonon suffers an intrinsic scattering during a time period Δt is thus

$$P_S = 1 - \exp(-\upsilon_g \Delta t/\Lambda) \tag{2}$$

where $\Lambda = \upsilon_g \tau$ is the phonon mean free path.

2.2 Gray medium approximation

In the present study, the media are assumed to be gray; that is phonon properties are averaged over frequency. The temperature dependence of these average properties relies on the adopted phonon dispersion relation. In the present study, we adopt the experimentally measured one (www.ioffe.rssi.ru/SVA/NSM /Semicond/) for bulk Si and Ge. Note the size confinement effect on the phonon dispersion relation is not considered because it is a minor effect compared to the interface scattering effect. Besides, the phonon dispersion relation is assumed to be isotropic and as the same as that in the 100 direction. When a system is at equilibrium at a temperature T, its energy per unit volume and specific heat are

$$U = \sum_p \int_0^{k_B\theta_{D,p}/\hbar} n_0 \hbar\omega \cdot D(\omega)\, d\omega \tag{3}$$

and

$$C = \sum_p \int_0^{k_B\theta_{D,p}/\hbar} \frac{\partial n_0 \hbar\omega}{\partial T} \cdot D(\omega)\, d\omega \tag{4}$$

where k_B and $\hbar$ are Boltzmann constant and Plank constant divided by 2π; ω is the phonon frequency; $\theta_{D,p}$ is the Debye temperature for the p^{th} polarization; $D(\omega) =$

$q^2\partial q/2\pi^2\partial\omega$ is the phonon density of states, and n_0 is the equilibrium phonon distribution, namely $n_0 = 1/(\exp(\hbar\omega/k_BT) - 1)$. The total number of phonons per unit volume ($\bar{n}$), the average phonon energy ($\hbar\bar{\omega}$), and the average phonon group velocity ($\bar{\upsilon}_g$) are now defined respectively as

$$\bar{n} = \sum_p \int_0^{k_B\theta_{D,p}/\hbar} n_0 D(\omega)\, d\omega \tag{5}$$

$$\hbar\bar{\omega} = U/\bar{n} \tag{6}$$

and

$$\bar{\upsilon}_g = \frac{1}{C}\sum_p \int_0^{k_B\theta_{D,p}/\hbar} \frac{\partial\omega}{\partial q}\frac{\partial n_0\hbar\omega}{\partial T}\cdot D(\omega)\, d\omega \tag{7}$$

Note herein we propose a specific-heat-weighted averaged phonon group velocity instead of the phonon population (Jeng, Yang, Song, and Chen, 2008), because from the kinetic theory the lattice thermal conductivity is related to the phonon mean free path, the specific heat, and the group velocity by

$$k_{bulk} = \frac{1}{3}C\bar{\upsilon}_g\Lambda \tag{8}$$

In fact, Equation (8) is also used to compute the overall phonon mean free path based on the experimentally measured bulk thermal conductivities (Glassbrenner and Slack, 1964).

A table of these temperature-dependent properties is thus pre-prepared and linear interpolations are employed whenever phonon properties at some temperature are required during the simulation.

2.3 Transmission models

When a phonon hits a Si/Ge interface, it may be transmitted or reflected, diffusely or specularly. A parameter p, the specular fraction, is usually employed to characterize the roughness of the interface and is defined as the fraction of phonons that are specularly transmitted or reflected. We compute the specular transmissivity according to the inelastic acoustic mismatch model proposed by Chen (1998) as follows

$$\tau_{12} = \frac{4Z_1Z_2\cos\theta_1\cos\theta_2}{(Z_1\cos\theta_1 + Z_2\cos\theta_2)^2} \text{ for } 0 \le \theta_1 < \theta_{cr} \tag{9}$$

and $\tau_{12} = 0$ for $\theta_{cr} \leq \theta_1 < \pi/2$, where θ_1 is the incident angle and $Z = \rho \bar{v}_g$ is the acoustic impedance (ρ is the density). Besides, the transmitted angle θ_2 is determined by

$$\frac{\sin\theta_2}{\sin\theta_1} = \sqrt{\frac{U_1 \bar{v}_{g,1}}{U_2 \bar{v}_{g,2}}} \tag{10}$$

From Equation (10), the critical angle θ_{cr} for full reflection is thus

$$\sin\theta_{cr} = \sqrt{\frac{U_2 \bar{v}_{g,2}}{U_1 \bar{v}_{g,1}}} \tag{11}$$

On the other hand, if a phonon is diffusely transmitted or reflected, we compute the associated transmissivity as

$$\tau_{12} = \frac{U_2 \bar{v}_{g,2}}{U_1 \bar{v}_{g,1} + U_2 \bar{v}_{g,2}} \tag{12}$$

When there is a nonzero heat flux, a temperature jump is expected across a heterogeneous interface. Because of the hyperbolic characteristic of the PBTE, we propose to evaluate these transmissivities at the temperature on the incident side. In other words, all variables in Equations (9)$\sim$(12) are evaluated at the instantaneous temperature on the incident side. Consequently, when the interface is totally diffuse for instance, the net energy flux across the interface is estimated to be

$$q_{1\to 2} = f(T_1) - f(T_2) \tag{13}$$

$$f(T) = \frac{1}{4} \cdot \frac{U_1(T)\,\bar{v}_{g,1}(T)\,U_2(T)\,\bar{v}_{g,2}(T)}{U_1(T)\,\bar{v}_{g,1}(T) + U_2(T)\,\bar{v}_{g,2}(T)} \tag{14}$$

where T_1 and T_2 are the temperatures on the two sides of an interface. It can be shown that the function $f(T)$ is a monotonically increasing function of temperature T. Therefore, heat flows from side 1 to side 2 when $T_1 > T_2$ and a thermal equilibrium is reached when $T_1 = T_2$.

3 Monte-Carlo solver

We are now ready to develop a MC tool for solving the PBTE based on the physical models described in the previous section. To begin with, the system of interest is divided into many cells as illustrated in Fig.1 (distinguished by the dotted lines). Each cell is constituted of one material (called "cell material"). A heterogeneous interface thus exists between two neighboring cells if the cell materials are different.

Initially, phonons are randomly uniformly distributed within each cell according to the given temperature and the cell material. Each phonon possesses an energy of either $\hbar\bar{\omega}_{Si}$ or $\hbar\bar{\omega}_{Ge}$ and flies in a uniformly random direction. For the sake of having a reasonable computational amount, phonons are sometimes grouped as bundles; a "simulated phonon" actually represents a bundle of phonons. The number of phonons per bundle (W) is chosen to be the same for both Si and Ge in all the following simulations.

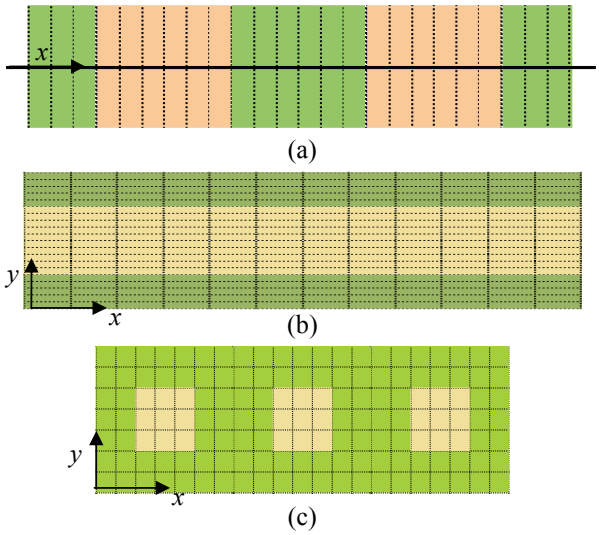

Figure 1: The 1D (a) and 2D (b,c) grid systems employed for phonon transport in a superlattice thin film and a compact material embedded with regularly aligned square nanowires.

3.1 Operator splitting

We adopt the operator splitting technique as usual. Phonons are first drafted at their instantaneous group velocity. A uniform random number between 0 and 1 is then drawn for each phonon. If this random number is less than P_S, the phonon is judged to suffer an intrinsic scattering: its moving direction is randomly reassigned and other properties are made to comply with the local temperature. To conserve the total energy, the energy imbalance due to scattering is traced for each cell. A phonon will be added to or deleted from the cell whenever the amount of the energy imbalance exceeds half the energy per phonon bundle at the local temperature.

A judgment is made whether a phonon reaches the cell boundary on the way of its flight. If yes, the cell boundary is examined whether it is a heterogeneous interface (whether the cell materials on the two sides of the cell boundary are different). If yes again, two uniform random numbers, r_1 and r_2, between 0 and 1 are drawn. When $r_1 < p$, the phonon will be specularly transmitted ($r_2 < \tau_{12}$) or reflected ($r_2 > \tau_{12}$); otherwise, it will be diffusely transmitted ($r_2 < \tau_{12}$) or reflected ($r_2 > \tau_{12}$). The moving direction of the phonon must be changed accordingly (specularly or diffusely) and its group velocity is updated according to the new cell material. Furthermore, we keep the energy of the phonon unchanged, no matter it is transmitted or reflected, specularly or diffusely, in order to be consistent with the inelastic acoustic mismatch model. Consequently, phonons in a cell may carry an energy of either $\hbar\bar{\omega}_{Si}$ or $\hbar\bar{\omega}_{Ge}$, regardless of the cell material. To distinguish them, we attach one additional property to each phonon, named "the energy material" Si (or Ge) if its energy is $\hbar\bar{\omega}_{Si}$ (or $\hbar\bar{\omega}_{Ge}$).

3.2 Symmetry condition

The computational amount can be significantly reduced by taking advantage of geometric symmetry. For instance, the phonon transport in the cross-plane (x) direction of a superlattice thin film, as shown in Fig.1a, can be modeled as a one dimensional problem, because due to the symmetry the probability of finding a phonon locating at (x,y,z) is as the same as that at (x,0,0). We can, from the statistical viewpoint, replace a phonon located at (x,y,z) by one having exactly all the same properties but located at (x,0,0). Therefore, although phonons are moving in a three dimensional space, only the x coordinate needs time-marching and recording and consequently a one dimensional grid system is sufficient.

Two two-dimensional examples are the in-plane ($x-z$) phonon transport in a superlattice thin film and the cross-wire phonon transport in a compact material embedded with regularly aligned nanowires as shown in Figs.1b and 1c (Yang and Chen, 2004; Yang, Chen, and Dresselhaus 2005). Supposed heat flows in the x-direction, the probability of finding a phonon locating at (x,y,z) is as the same as that at (x,y,0) so that we can replace a phonon located at (x,y,z) by another one located at (x,y,0).

3.3 Numerical boundary conditions

We prefer a prescribed heat flow rate in the system instead of prescribed boundary temperatures because the temperature on the boundary cross section is usually not uniform. In order to maintain a steady heat flow rate in the system, phonons must be injected into the domain from the boundaries. Due to the existence of nanostructures, the heat flux is again usually non-uniform and phonons leaving the computational domain very likely possess directional dependence. Boundary conditions

that are inconsistent with either one could cause inaccurate or even unreasonable results. The pseudo-periodic boundary condition proposed by Jeng, Yang, Song, and Chen (2008) is a good choice but not sufficiently accurate. We thus propose a modified one herein. Like what they did, data sets $pool(s,j,k)$ are built at each time step that record the moving directions, locations, remaining flight time, and "energy material" of leaving phonons from the cell (s,j,k), where s=1 or N_x represents the left or right boundary. The total energy leaving the computational domain from the cell (s,j,k) and the net amount of heat flowing across some referenced cross section during one time step Δt are also recorded and denoted as $E(s,j,k)$ and $q(r,j,k)$ respectively (r represents the referenced plane). The total amounts of energies that should be injected into the cell (s,j,k) from the boundaries at next time step are thus set to be equal to

$$J(s,j,k) = E(s,j,k) \pm \left(q(r,j,k) / \sum_{j,k} q(r,j,k) \right) Q_0 \Delta t \tag{15}$$

where + for s=1 and - for $s = N_x$, and Q_0 is the prescribed total heat flow rate. Instead of assuming a heat flux distribution proportional to $E(s,j,k)$ as done by Jeng, Yang, Song, and Chen (2008), we measure and use the actual distribution on the referenced cross section. To be reasonable, the referenced and the boundary cross sections must be geometrically equivalent, for instance the middle plane in between two neighboring nanowires in Fig.1c. The profiles of $E(s,j,k)$ and $q(r,j,k)$ may be similar because they are both dominated by the layout of the nanostructures. They are not exactly the same nonetheless because $E(s,j,k)$ represents energy flux coming from one side of a cross section and is determined mainly by the local temperature while $q(r,j,k)$ instead is dominated by the temperature gradient. A comparison of them obtained from a two-dimensional simulation of in-plane phonon transport in a Si(100nm)/Ge(100nm) superlattice thin film is shown in Fig.2 ($E(s,j)$ and $q(s,j)$ for the 2D case). It is found the actual heat flux is particularly low near the totally diffuse interfaces (p=0). Without these dips near the interfaces, the old method (a heat flux distribution proportional to $E(s,j,k)$) generates unexpected temperature jumps across the interfaces and thus an unwanted heat transfer in the y direction.

Phonons to be injected from one boundary are then randomly selected from the data set $pool(s,j,k)$ collected on the other boundary. Attached by the energy per phonon bundle of the recorded "energy material" and the group velocity of the cell material at the instantaneous boundary temperature, phonons are injected into the computational domain from the recorded positions and directions and drafted for the recorded remaining flight time. The total amount of energy injected must be as close to $J(s,j,k)$ as possible. Any energy imbalance at the boundaries is again

recorded and is to be complemented in next time step. The importance of the use of the property "energy material" will be highlighted in the subsection 4.2.2.

4 Simulation results

The validity and accuracy of the proposed MC solver are tested in this section. We first test it with a simple one-dimensional transient problem and then apply it to simulate the cross-plane (1D) and in-plane (2D) phonon transport phenomena in a Si/Ge superlattice thin film. The simulation results will be compared with theoretical predictions. The proposed MC solver can be easily applied to 3D problems by giving up the symmetry condition. The related simulation results are not shown herein because the authors would like to highlight the advantage of using the symmetry condition.

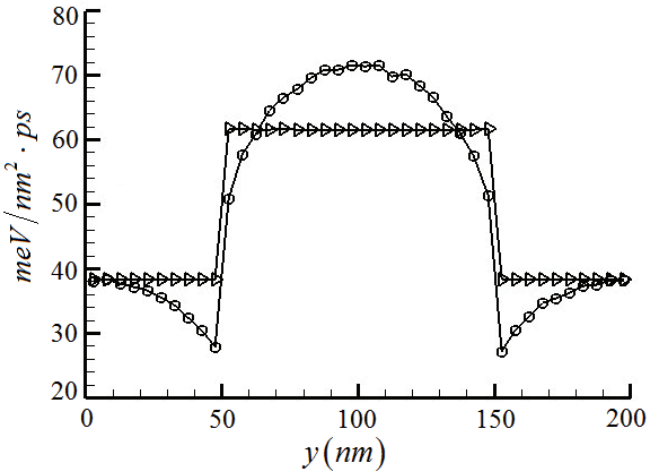

Figure 2: A comparison of the imposed heat flux distributions at the boundaries according to $E(s,j)$ (triangles) and $q(r,j)$ (circles).

4.1 Transient thermal conduction

The thermal diffusion problem of a thermally insulated bulk silicon, which is initially 200K on the left half part and 400K on the right half part, is simulated and the results are shown in Fig.3. A finite-difference solution is also obtained by solving the transient diffusion equation

$$\frac{\partial U}{\partial t} = \frac{\partial}{\partial x}\left(k_{bulk}\frac{\partial T}{\partial x}\right) \tag{16}$$

where the temperature dependences of the thermal conductivity and the internal energy U are taken from the MC simulation. It is seen the MC solution diffuses slower than the finite-difference solution at very early times. This is because unlike the immediate diffusion assumed in the traditional diffusion equation, it takes time for phonons to draft in a MC simulation. As time increases, after phonons have suffered many enough scatterings, the difference between the two solutions disappears gradually.

4.2 Cross-plane phonon transport

As discussed before, the cross-plane phonon transport in a superlattice thin film is a statistically one dimensional problem and thus the cells are in a line. Phonons are still moving in a three dimensional space but whenever a phonon leaves the x-axis, it is replaced by one located at (x,0,0) carrying all the same properties. In other words, only the x-coordinates of the phonons need being time-marched and recorded in the computer memory. The cross-sectional area A serves as a free parameter that can be adjusted to control the number of phonons per bundle.

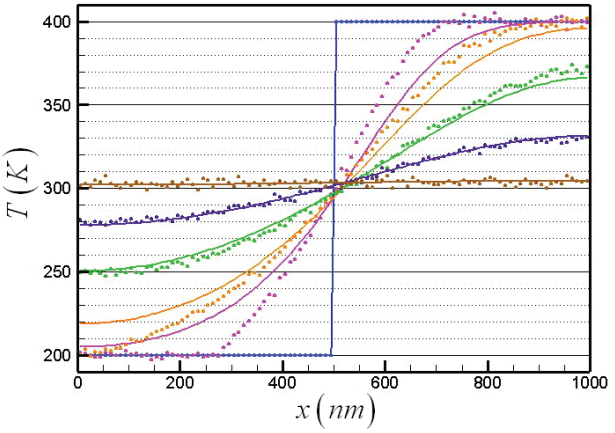

Figure 3: The temperature evolution obtained by a MC solver (symbols) and a finite-difference scheme (lines) at t= 0, 40, 120, 400, 900, and 3000ps.

4.2.1 Theoretical analysis

We attempt to compare the simulation results with the predictions by Chen (1998), in which the PBTE is solved analytically also under the single-relaxation-time approximation and the gray-medium approximation. Several differences are nonetheless existent between this analysis and the simulation. In Chen's analysis, the

phonon properties such as the acoustic specific heat (C), the group velocity (υ_g), and the mean free path (Λ) are all assumed to be constant and have their values at 300K; the interface thermal resistances are all assumed to be the same; the transmissivities are calculated in use of specific heat instead of internal energy and consequently they are temperature-independent. The last difference results in not only different values of transmissivities but also different critical angles for full reflection. In short, Chen's model counts the temperature gradient effect but not the temperature dependence of all phonon properties except the energy.

4.2.2 Directional dependence

Before investigating the heat transfer in a superlattice thin film, we explore the directional dependence of phonons that is very likely existent due to the interface scattering and the spectral responses of transmission/reflection. This directional dependence is expected particularly strong when the phonon transport is in ballistic regime and must be carefully implemented into the numerical boundary conditions.

We investigate the directional dependence in an insulated Si(25nm)/ Ge(25nm) superlattice thin film, which is in equilibrium at 300K. Six periods are simulated. The directional distributions of the energy and the number of phonons incident on the middle plane of each Si layer from both sides are collected and shown in Fig.4, in which $\mu = \cos\theta$ and θ is the angle between the phonon moving direction and the x-axis. It is found regardless of specular or diffuse interfaces, the incident energy distribution is always linear, implying the system does remain at equilibrium. On the other hand, the directional pdf (probability density function) of the phonon population is nearly linear when p=0 except a short parabola near the origin but an obvious jump is observed at the critical angle ($\mu_{cr} \approx 0.57$) when p=1. This jump arises from the fact that $\hbar\bar{\omega}_{Si}$ is greater than $\hbar\bar{\omega}_{Ge}$ and the fact that there are only Si phonons below μ_{cr} (all transmitted Ge phonons are confined within the cone $\mu > \mu_{cr}$). The magnitude of the jump decreases with decreasing specular fraction p and increasing layer thickness d as shown in Fig.5, because of increasing interface or intrinsic scatterings. Such a directional dependence must be preserved when phonons are injected from the boundaries. The pseudo-periodic boundary condition discussed in Sec. 3.3 must and should be able to capture it automatically via the use of the property "energy material". However, the limited size of the data pools may cause a failure. Noticing the directional dependence is much weaker in the Ge layers (the layer in which no full reflection occurs), we choose Ge to be the material of the boundary cells. In all the followings, simulations are thus so performed.

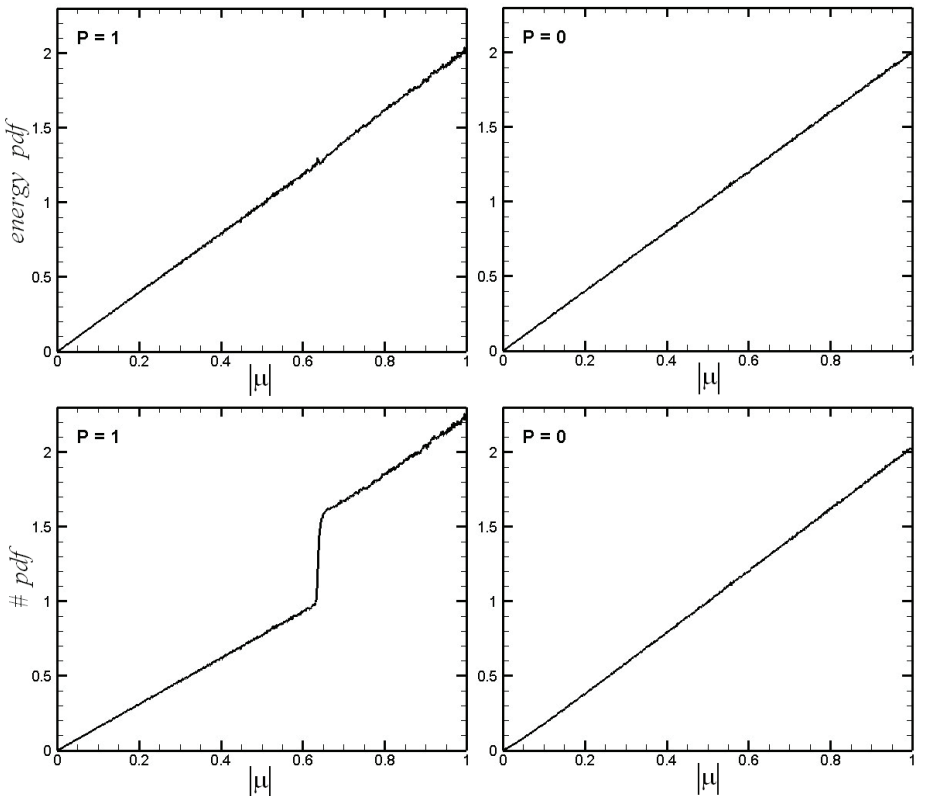

Figure 4: The directional probability density functions of phonon numbers and energy.

4.2.3 Number of simulated periods

To further reduce the possible contamination due to the numerical boundary conditions, sufficiently many periods should be simulated for each specimen. Figure 6 shows the computed thermal conductivity of a Si(25nm)/Ge(25nm) superlattice thin film, compared with the analytical prediction against the number of simulated superlattice periods. In these calculations, numerical parameters employed are Δx=2.5nm, Δt=0.25ps, and A=10nm^2. The prescribed heat flow rate are $Q_0/\Delta t = 10$ and $20 meV/nm^2 \cdot ps$ for p=0 and 1 respectively. Initially the temperature is 330K and 1944 and 1000 phonon bundles are placed within each Ge cell and each Si cell respectively. The lattice thermal conductivity is obtained according to the Fourier's law and based on the temperature difference across the middle superlattice period (labeled by "mid") or the whole computational domain (labeled by

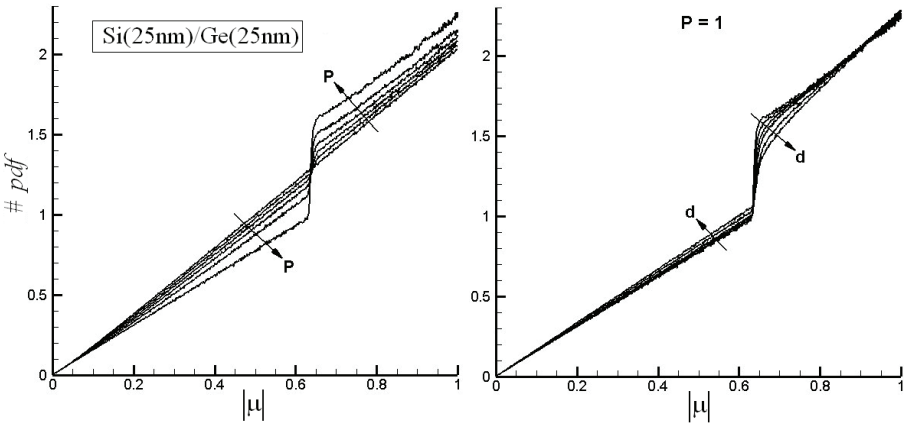

Figure 5: The directional probability density functions of phonon numbers in a Si(d)/Ge(d) superlattice thin film. The arrows indicate the increasing direction of the relevant parameter.

"total"). Several temperature distributions are also shown in Fig.7 for illustration. Figure 6 shows the computed thermal conductivity is nearly independent of the number of simulated superlattice periods, implying the proposed pseudo-periodic boundary condition works very successfully.

4.2.4 Interface roughness and superlattice period

We are now ready to study the dependence of the lattice thermal conductivity of a Si(d)/Ge(d) superlattice thin film on the interface roughness (p) and the superlattice period ($2d$). The computational domain for each case is chosen to be two periods. The computed thermal conductivities agree excellently with the analytical predictions as seen in Fig.8 and Fig.9. The temperature jumps at the four interfaces are only slightly different, although they are larger across the Si-Ge interfaces than across the Ge-Si interfaces in all cases.

4.3 In-plane phonon transport

We now consider the situation in which the main heat flow direction is one (x) of the in-plane directions of a superlattice thin film. It is reasonable to assume the phonon statistics is the same along the other in-plane direction (z) and thus 2D simulations are wanted. The grid system as shown in Fig.1b is employed. The periodic boundary condition is imposed in the y-direction; that is, whenever a phonon leaves the computational domain from the top (bottom) surface, it will immediately

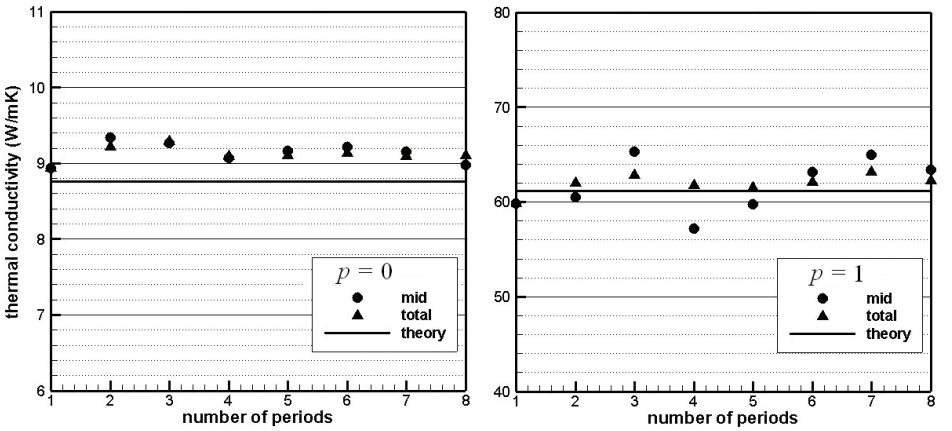

Figure 6: The computed cross-plane thermal conductivities of a Si(25nm)/Ge(25nm) superlattice thin film against the number of superlattice periods simulated.

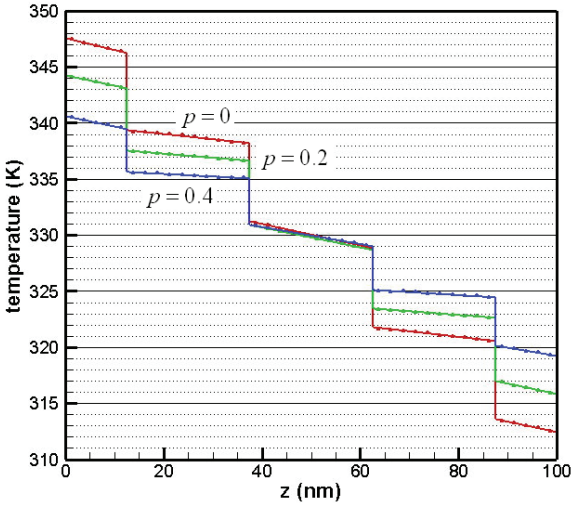

Figure 7: The temperature distribution in a two-period specimen of a Si(25nm)/Ge(25nm) superlattice thin film.

re-enter the computational domain from the bottom (top) surface. The pseudo-periodic boundary condition on the other hand is imposed in the x-direction. It is the width w now that serves as a free parameter to control the number of phonons

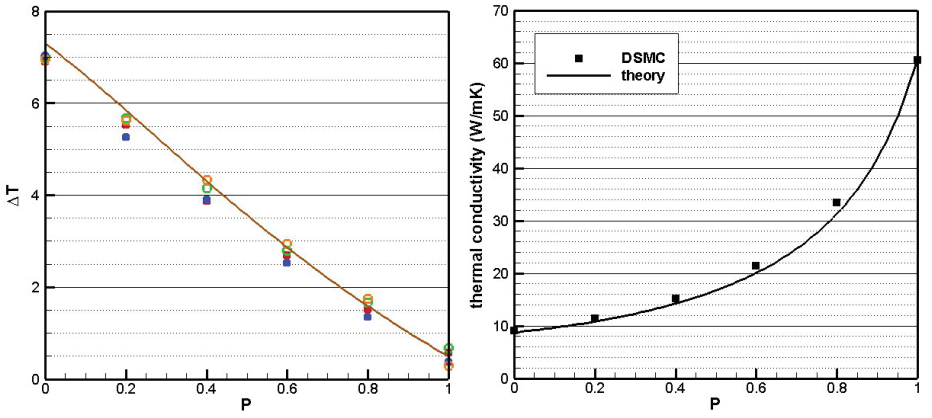

Figure 8: The temperature jumps at the Ge-Si (solid symbols) and Si-Ge (open symbols) interfaces and the cross-plane thermal conductivity of a Si(25nm)/Ge(25nm) superlattice thin film against the interface roughness.

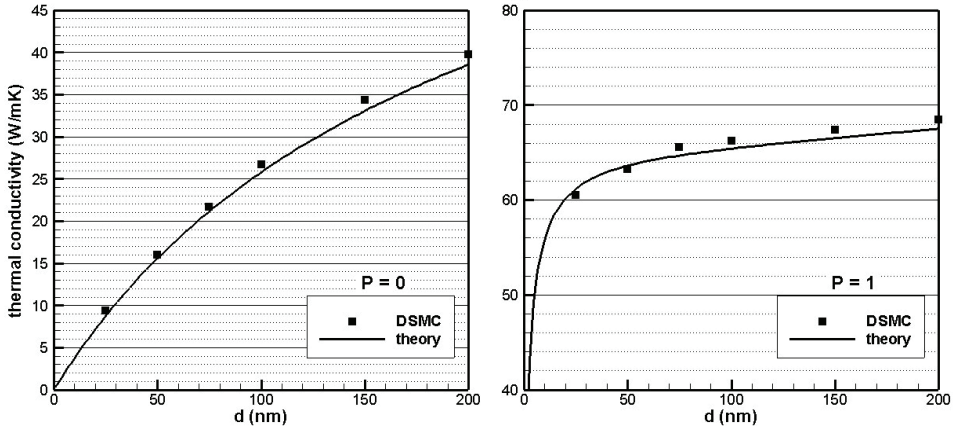

Figure 9: The cross-plane thermal conductivity of a Si(d)/Ge(d) superlattice thin film against the film thickness d.

per bundle.

4.3.1 Theoretical analysis

An analysis similar to that done by Chen (1997) is performed to predict the in-plane thermal conductivity. In the analysis, a linear dispersion relation and Holland's model (Holland, 1963) for the frequency- and temperature-dependent relax-

ation time are employed. Unlike the MC simulations, the elastic acoustic mismatch model is used for the spectral transmissivity, which is also frequency-dependent. Full reflection occurs not only when the incident angle is larger than the critical angle but also when the incident frequency is larger than the Debye frequency on the transmitted side. Most of all, diffusely scattered phonons are assumed to be in equilibrium with the local temperature and make no contribution to the heat transfer. This is not true in the simulations, in which a nonzero net heat flow rate, proportional to $f(T_1) - f(T_2)$, is allowed when the interface is totally diffuse. Consequently, the bulk thermal conductivities calculated based on this theoretical model are 149.35W/mK and 69.76W/mK at 300K for Si and Ge respectively, slightly different from the experimentally measured ones (156W/mK and 60W/mK). A poorer agreement between the analytical predictions and simulation results is thus expected.

4.3.2 Length of simulated domain

Because of the co-existence of two different materials on the cross section, a directional dependence of the phonon population and a non-uniform cross-sectional distribution of heat flux are expected, particularly when the interface is very smooth or the layer thickness is very small. We thus test the validity of the proposed pseudo-periodic boundary condition by varying the length (L) of the computational domain of a Si(2nm)/Ge(2nm) superlattice thin film with perfectly specular interfaces. The middle cross section at $x = L/2$ is selected as the reference plane for capturing the heat flux distribution. To avoid a too large temperature difference, the specified heat flow rate cannot be too large; consequently, the collected instantaneous heat flux distribution may fluctuate violently. To solve this problem, we average the heat flux distribution over several thousands of previous time steps and impose the result at the boundaries. Figure 10 shows the simulation results at 300K (initial temperature). It is seen the heat flux is larger in the Si layer because its bulk thermal conductivity is larger. When the length of the sample is not long enough, unreasonable temperature jumps are observed across the heterogeneous interfaces near the inlet and outlet boundaries (not shown herein), resulting in a smaller thermal conductivity. The situation gets improved as L increases. In this special case, Si(2nm)/Ge(2nm) and p=1, L=400 nm is seemingly necessary for a convergence of the thermal conductivity.

4.3.3 Interface roughness and superlattice period

After carefully testing and choosing the numerical parameters, we investigate the dependence of the in-plane thermal conductivity of a Si(d)/Ge(d) superlattice thin film on the interface roughness and the superlattice period. The simulation results

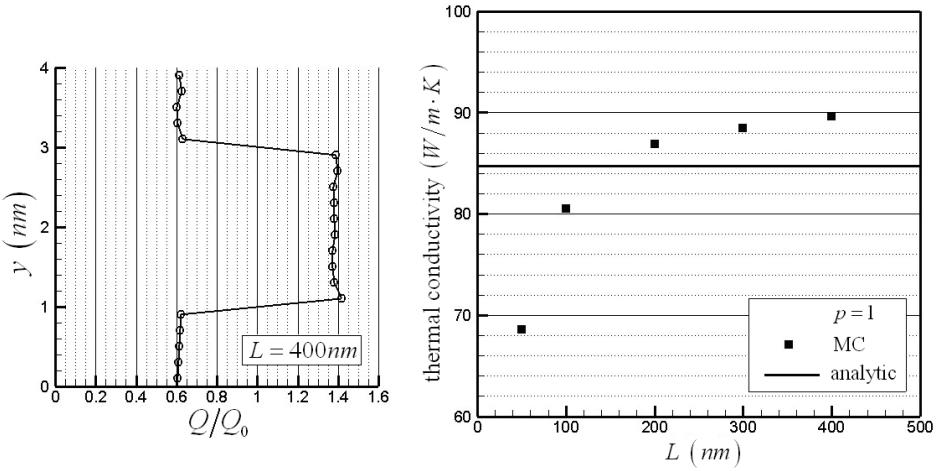

Figure 10: The heat flux distribution and the in-plane thermal conductivity of a Si(2nm)/Ge(2nm) superlattice film against the length of the simulated sample.

are shown in Fig.11, compared with the analytical predictions. Some differences are observed. Because the agreement is better when the interfaces are smooth or when the layer thickness is small, it is conjectured the deviation arises from the ignorance of the contribution of the diffusely scattered phonons to the heat transfer in the theoretical analysis. Besides, the computed thermal conductivities with p=1 are slightly larger than the predictions. This is attributed to the larger bulk thermal conductivity of Si used in the MC simulations. Finally, it is very surprising to see that the simulation data collapse very well with the theoretical curves at lower temperatures (320K for p=1 and 236K for p=0) than the initial one (330K). It implies both the simulation and the theoretical models capture the size effect in a similar way, although there are some differences in the physical models.

4.3.4 Ratio of layer thicknesses

It is believed the ratio of the layer thicknesses also plays an important role in the in-plane phonon transport, because the thermal resistances of layers are connected in parallel now. In spite of having a larger bulk thermal conductivity, the Si layer may have a larger thermal resistance when its thickness is too thin (implying not only a too small cross sectional area but also enhanced interface scatterings). We show in Fig.12 the heat flux distributions over the thickness direction associated with a Si(d_{Si})/Ge(d_{Ge}) superlattice thin film with p=0 and a fixed period of $d_{Si} + d_{Ge} = 20nm$. It is observed the layer taking care of the major part

of heat transfer is changed from the Si layer (the middle layer) to the Ge layer as d_{Si}/d_{Ge} gradually decreases. The computed in-plane thermal conductivity against the thickness ratio is shown in Fig.13. Again, it is seen the simulation data collapses very well with the theoretical prediction at a lower temperature than the prescribed one (330K). Interestingly, there exists an optimum ratio that results in a minimum in-plane thermal conductivity. If the interface scattering is ignored, the effective in-plane thermal conductivity of a Si(d_{Si})/Ge(d_{Ge}) superlattice thin film should be $k_{eff} = (k_{Si}d_{Si} + k_{Ge}d_{Ge})/(d_{Si} + d_{Ge})$, which is a monotonically increasing function of d_{Si}/d_{Ge} because $k_{Si} > k_{Ge}$. The existence of the minimum conductivity therefore must arise from the interface scattering and can be explained by a competition between the reducing interface scattering and the increasing intrinsic scattering in the Ge layer as d_{Si}/d_{Ge} decreases. This explanation is supported by the observation also from Fig.13 that the larger the superlattice period or the larger p (i.e. the less important the interface scattering), the smaller the optimum ratio d_{Si}/d_{Ge} is.

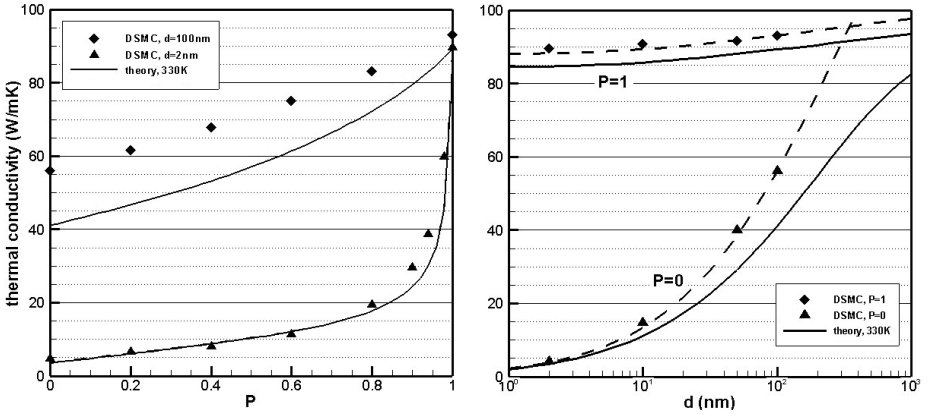

Figure 11: The computed in-plane thermal conductivity of a Si(d)/Ge(d) superlattice thin film. The dash lines are the theoretical predictions at 320K for p=1 and 236K for p=0.

5 Conclusions

We have established a quick MC simulation tool for analyzing the phonon transport phenomenon in nanostructured materials. Geometric symmetries that exist in the systems are employed to reduce the dimension in problem and consequently the computational amount. The MC tool is thus identified as a 1D, 2D, or 3D solver. A quasi-periodic boundary condition is properly designed to generate a prescribed

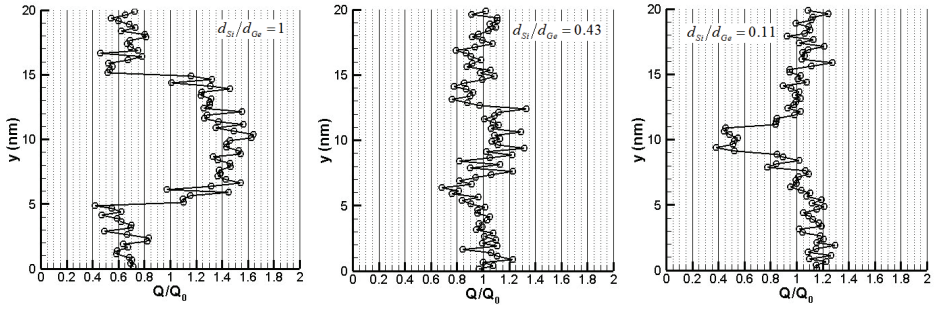

Figure 12: The heat flux distributions for a Si(d_{Si})/Ge(d_{Ge}) superlattice thin film with p=0 and a fixed period of $d_{Si}+d_{Ge}=20nm$.

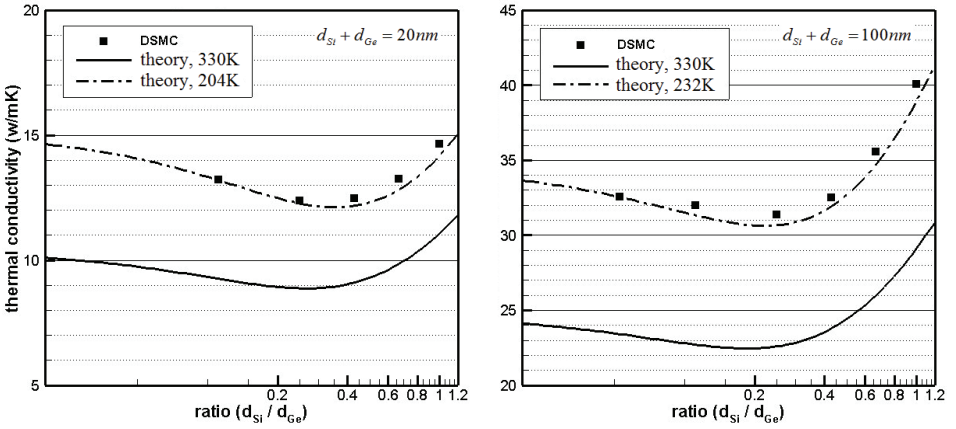

Figure 13: The in-plane thermal conductivity against the layer thickness ratio for superlattice thin films having a fixed superlattice period, $d_{Si}+d_{Ge}$, and p=0.

heat flow rate in the system, which is capable of capturing the directional dependence of phonon populations and the non-uniformity of the heat flux distribution due to the existence of the heterogeneous interfaces. We have successfully verified the validity and accuracy of the proposed MC solver by applying it to a 1D transient conduction problem and the cross-plan and in-plane phonon transports in Si/Ge superlattice thin films. The simulation results show good agreement with theoretical predictions, in spite of slight differences which can be reasonably explained by the discrepancies in the physical models between the simulation and the analysis. The simulation results also indicate the cross-plane thermal conductivity of a Si/Ge superlattice thin film increases monotonically with the smoothness of the interfaces

and the superlattice period. A minimum value on the other hand is found associated with the in-plane thermal conductivity of a Si/Ge superlattice thin film as the ratio of the layer thicknesses is varied and the superlattice period is fixed. This may be explained by a competition between the decreasing interface scattering and the increasing intrinsic scattering with the increasing Ge-layer thickness.

Acknowledgement: This work was supported by the Industrial Technology Research Institute of Taiwan, R.O.C (project No. 97-S-A24) as well as by the National Science Council of Taiwan (Grant No. NSC 97-2221-E-002-200-MY3).

References

Balandin, A.; Wang, K. L. (1998): Significant decrease of the lattice thermal conductivity due to phonon confinement in a free-standing semiconductor quantum well. *Phys. Rev. B*, vol.58, pp.1544-1549.

Chen, G. (1997): Size and interface effects on thermal conductivity of superlattices and periodic thin-film structures. *J. Heat Transfer*, vol.119, pp.220-229.

Chen, G. (1998): Thermal conductivity and ballistic-phonon transport in the cross-plane direction of superlattices. *Phys. Rev. B*, vol.57, pp.14958-14973.

Chen, Y.; Li, D.; Lukes, J.R.; Majumdar, A. (2005): Monte Carlo simulation of silicon nanowire thermal conductivity. *J. Heat Transfer*, vol,127, pp.1129-1137.

Dresselhaus, M.S.; Chen, G.; Tang, M.Y.; Yang, R.; Lee, H.; Wang, D.; Ren, Z.; Fleurial, J.P.; Gogna, P. (2007): New directions for low-dimensional thermoelectric materials. *Adv. Mater.*, vol. 19, pp.1043-1053.

Escobar, R.A.; Ghar, S.S.; Jhon, M.S; Amon, C.H. (2006): Multi-length and time scale thermal transport using the lattice Boltzmann method with application to electronics cooling. *International Journal of Heat and Mass Transfer*, vol.49, pp.97-107.

Evgrafov A.; Maute K.; Yang R.G.; Dunn M.L. (2009): Topology optimization for nano-scale heat transfer, *International Journal for Numerical Methods in Engineering*, vol. 77, pp. 285–300.

Glassbrenner, C. J.; Slack, G. A. (1964): Thermal conductivity of silicon and germanium from 3˚K to the melting point. *Physical Review*, vol.134, pp.A1058-A1069.

Gomes, C.J.; Madrid, M.; Goicochea, J.V.; Amon C.H. (2006): In-plane and out-of-plane thermal conductivity of silicon thin films predicted by molecular dynamics, *Journal of Heat Transfer*, vol.128, pp.1114-1121.

Hochbaum, A.; Chen, R.; Delgado, R.D.; Liang, W.; Garnett, E.C.; Najarian,

M.; Majumdar, A.; Yang, P. (2008): Enhanced thermoelectric performance of rough silicon nanowires. *Nature*, vol.451, pp.163.

Hoover, W.G. (1983): Nonequilibrium molecular dynamics, *Ann. Rev. Phys. Chem.*, vol.34, pp.103-127.

Huang, M.J.; Chong, W.Y.; Chang, T.M. (2006): The Lattice Thermal Conductivity of a Semiconductor Nanowire. *J. Applied Physics*, vol.99, 114318.

Huang, M.J.; Chang, T.M. ; Chong, W.Y. (2007): A New Lattice Thermal Conductivity Model of a Thin Film Semiconductor. *International Journal of Heat and Mass Transfer*, vol.50, pp.67-74.

Hyldgaard, P.; Mahan, G.D. (1996): Phonon Knudsen flow in GaAs/AlAs superlattices. *Thermal Conductivity*, vol.23, pp.172-182.

Jeng, M.S.; Yang, R.; Song, D.; Chen, G. (2008): Modeling the thermal conductivity and phonon transport in nanoparticle composites using Monte Carlo simulation. *Journal of Heat Transfer*, vol.130, 042410.

Khitun, A.; Balandin, A.; WANG, K. L. (1999): Modification of the lattice thermal conductivity in silicon quantum wires due to spatial confinement of acoustic phonons. *Superlattices and Microstructures*, vol.26, pp.181-193.

Kiselev, A.A.; Kim, K.W. (2000): Thermal conductivity of Si/Ge superlattices: a realistic model with a diatomic unit cell. *Phys. Rev. B*, vol.62, pp.6896-6899.

Lacroix, D.; Joulain, K.; Lemonnier, D. (2005): Monte Carlo transient phonon transport in silicon and germanium at nanoscale. *Phys. Rev. B*, vol.72, 064305.

Mazumder, S.; Majumdar, A. (2001): Monte Carlo study of phonon transport in solid thin films including dispersion and polarization. *J. Heat Transfer*, vol.123, pp.749-759.

Murthy, J. Y.; Mathur, S. R. (2002): Computation of sub-micron thermal transport using an unstructured finite volume method, *ASME J. Heat Transfer*, vol. 124, pp.1176-1181.

Peterson, R.B. (1994): Direct simulation of phonon-mediated heat transfer in a Debye crystal. *J. Heat Transfer*, vol.116, pp.815-822.

Shen S.; Atluri S. N. (2004): Multiscale Simulation Based on The Meshless Local Petrov-Galerkin (MLPG) Method, *CMES: Computer Modeling in Engineering and Sciences*, vol. 5, p.235-255.

Tian W.; Yang, R. (2007): Thermal conductivity modeling of compacted nanowire composites. *J. Appl. Phys.*, vol.101, 054320.

Tian W.; Yang, R. (2008): Phonon Transport and Thermal Conductivity Percolation in Random Nanoparticle Composites, *CMES: Computer Modeling in Engi-*

neering and Sciences, vol. 24, p.123-141.

Venkatasubramanian, R.; Siivola, E.; Colpitts, T.; O'Quinn, B. (2001): Thin-film thermoelectric devices with high room-temperature Figures of merit. *Nature*, vol. 413, pp.597-602.

Volz, S.G.; Saulnier, J.B.; Chen, G.; Beauchamp, P. (2000): Computation of thermal conductivity of Si/Ge superlattices by molecular dynamics techniques, *Microelectronics Journal*, vol.31, pp.815-819.

Walkauskas, S.G.; Broido, D.A.; Kempa, K.K.; Reinecke, T.L. (1999): Lattice thermal conductivity of wires. *J. Appl. Phys.*, vol.85, pp.2579-2582.

Yang R.; Chen G. (2004): Thermal conductivity modeling of periodic two-dimensional nanocomposites, *Physical Review* B, vol.69, 195316.

Yang R.; Chen G.; Dresselhaus M.S. (2005): Thermal conductivity of simple and tubular nanowire composites in the longitudinal direction, *Physical Review* B, vol.72, 125418.

Yang, R.; Chen, G.; Laroche, M.; Taur, Y. (2005): Simulation of nanoscale multidimensional transient conduction problems using ballistic-diffusive equations phonon Boltzmann equation. *J. Heat Transfer*, vol.127, pp.298-306.

Ziman, J.M.(2001): *Electrons and phonons*. Oxford University Press, Clarendon.

Zou, J.; Balandin, A. (2001): Phonon heat conduction in a semiconductor nanowire. *J. Appl. Phys.*, vol.89, pp.2932-2938.